Journal of Food Measurement and Characterization
https://doi.org/10.1007/s11694-025-03482-5

ORIGINAL PAPER

Impact of ohmic heating conditions on the behavior of metallized flexible packaging

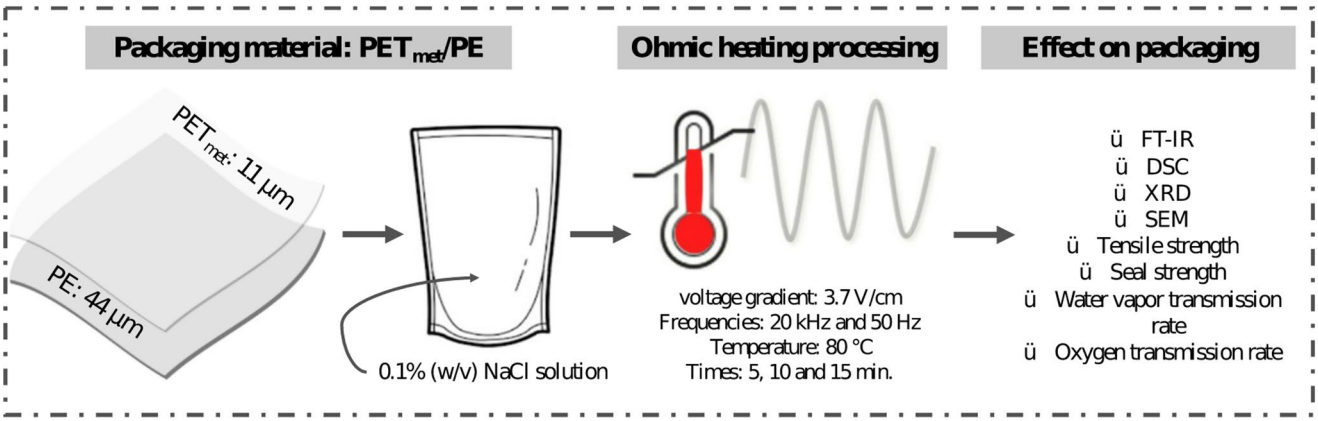
Luís Marangoni Júnior[1,2,3] · Rui M. Rodrigues[3,4] · Ricardo N. Pereira[3,4] · Danielle Ito[2] · Fábio Gomes Teixeira[2] · Marisa Padula[2] · António A. Vicente[3,4]

Received: 2 May 2025 / Accepted: 3 July 2025
© The Author(s), under exclusive licence to Springer Science+Business Media, LLC, part of Springer Nature 2025

Abstract

The integrity of packaging material is crucial for understanding the interactions among food, packaging, and processing, as it directly influences packaging performance, the efficacy of processing methods, and the stability of food. This study aimed to evaluate the effects of various ohmic heating (OH) processing conditions on the integrity of PET_{met}/PE films (PET: polyethylene terephthalate, met: metallization, and PE: polyethylene). OH processing was conducted on sealed packages containing a food simulant (0.1% (w/v) sodium chloride solution) with a voltage gradient of 3.7 V/cm and electrical frequencies of 20 kHz and 50 Hz. The target temperature was set at 80 °C, with holding times of 5, 10, and 15 min. The packages were assessed before and after OH processing concerning their structure and properties. The PET_{met}/PE films demonstrated no changes in chemical groups, thermal properties, or barrier properties related to water vapor and oxygen. However, the results show that OH processing caused measurable changes, such as a decrease in crystallinity from 21.4 to 14.8%. Mechanical properties like tensile and seal strength were also affected but remained within the typical range for such films, and the packaging integrity was preserved with no leaks. These minor variations do not compromise the material's performance, supporting its suitability for practical applications. Therefore, it can be concluded that PET_{met}/PE packaging is suitable for food products that will undergo OH processing under the conditions utilized in this research.

Graphical Abstract



Keywords Food thermal process · Emerging technology · Food packaging · Mechanical properties · Barrier properties

✉ Luís Marangoni Júnior
luismj@unicamp.br

[1] Department of Food Engineering and Technology, Scholl of Food Engineering, Universidade Estadual de Campinas (UNICAMP), Campinas, SP 13083-862, Brazil

[2] Packaging Technology Center, Institute of Food Technology, Campinas, São Paulo 13073-148, Brazil

[3] CEB– Centre of Biological Engineering, University of Minho, Campus de Gualtar, Braga 4710-057, Portugal

[4] LABBELS– Associate Laboratory, Braga, Guimarães 4710-057, Portugal

Published online: 11 July 2025

Introduction

Various food processing technologies are employed to ensure safety and extend the shelf life of products, particularly thermal pasteurization and sterilization methods. Changes in consumer lifestyles, partly due to globalization and health concerns, have significantly influenced eating patterns. Consequently, the scientific and industrial community is increasingly exploring new food processing technologies that have a lower environmental impact while delivering safer, more nutritious, convenient and high-sensory quality foods [1–3]. These innovative technologies can reduce processing time and energy consumption while better preserving nutrients in food [4, 5]. Moreover, they play a crucial role in the innovation of food products, leading to higher added value [6]. Examples of emerging food processing technologies currently being investigated include microwave heating, pulsed light, high pressure processing, ultrasound, and ohmic heating.

Among those emerging technologies, ohmic heating (OH) offers several advantages for food processing due to its rapid and uniform heating capabilities, in contrast to conventional heating methods that are constrained by convection and conduction heat transfer mechanisms [4, 7–9]. The fundamental principle of OH involves converting electrical energy into thermal energy, typically using an alternating current electric field, which provides high energy efficiency [3, 8–12]. OH facilitates the processing of a wide range of food systems, both particulate and non-particulate, potentially improving the quality of the final product. Notable applications of OH include blanching, evaporation, dehydration, fermentation, extraction, sterilization, and heating of foods [13]. Current research has demonstrated the successful application of this technology in processing fruits, vegetables, meat products, dairy products, and other foods, resulting in high-quality products [14].

While most applications thus far have targeted systems that require direct contact between food and processing equipment, OH of packaged foods is gaining consideration and has been explored in the scientific literature. For instance, OH post-pasteurization of vacuum-packed sausages has been proposed for effectively inactivating *Listeria monocytogenes*. Applying OH at 75 °C for 30 s resulted in a reduction of more than 5 logs of *L. monocytogenes*, without altering the chemical composition, pH, lipid oxidation, or water retention capacity of the sausage. These results highlight the potential of this technology for producing meat emulsions, ensuring food safety while minimally affecting the quality of the sausage [15].

Ohmic-assisted thermal sterilization (OATS) was utilized to validate the treatment of coconut milk. The coconut milk was packaged in PP/PA/PE (polypropylene/polyamide/polyethylene) bags and processed using OATS at 121.1 °C for 5 min, leading to the complete inactivation of *Clostridium sporogenes* spores, with only minor sensory changes in the product [16]. Additionally, orange juice packaged in a conductive PP film with carbon black was processed via OH. A temperature of 84 °C was measured at the geometric center when a voltage of 300 V was applied for 5 min, resulting in a 6-log reduction of *Escherichia coli*. This demonstrates the efficacy of OH for pasteurizing fruit juice [17].

Overall, the limited developments reported thus far regarding the processing of packaged foods via OH have mostly focused on the format of packaging materials, the coupling of electrodes, temperature distribution within the packaging, and the microbiological, physicochemical, and sensorial quality of processed foods [15–20]. In a previous study, we explored the impact of OH processing— employing a voltage gradient of 3.7 V/cm and a frequency of 20 kHz to achieve a thermal treatment of 80 °C for 1 min— on various food simulants and their effects on the properties of four multilayer flexible packaging materials (PET_{met}/PE, PET_{met}/PP, PET/Al/PE, and PET/Al/PA/PP) [21]. The interaction between the simulants and the packaging during processing led to significant alterations in the crystallinity, morphology, mechanical properties, and barrier performance of the metallized films in contact with acidic food simulants. Consequently, this research suggests the need to expand investigations into the effects of OH processing on the characteristics of flexible packaging, especially considering the impact of varying OH processing conditions on material integrity and interaction with food. Specifically, processing time and electrical variables, such as frequency, can profoundly influence the formation of radical species, electrode oxidation, and secondary reactions within the processing media and packaging, which may alter product safety and quality [12]. Therefore, this research focuses on a flexible packaging material that is commonly used for packaging foods subjected to processing with the pack or hot-filled.

PET_{met}/PE flexible multilayer packaging (PET: polyethylene terephthalate, met: metallization and PE: polyethylene) produced through lamination is widely utilized for packaging thermo-processed foods such as juices, pulps and sauces. PET is chosen for its abrasion resistance and excellent optical properties, while aluminum metallization provides effective gas and vapor barrier. PE is often selected for its superior sealing capabilities and water vapor barrier properties [22–24]. The aim of this research was to assess the effects of various OH processing conditions—specifically, electrical frequencies of 20 kHz and 50 Hz, a target temperature of 80 °C, and holding times of 5, 10, and 15 min—on the structure and properties of PET_{met}/PE packaging. The selection of 50 Hz and 20 kHz frequencies was

guided by their established use in both commercial applications and scientific research, representing low and high-frequency regimes that significantly influence electrolytic reactions and electrode stability. The innovative aspect of this study lies in examining the interplay between adjustable OH processing conditions and packaging performance, which can lead to enhanced food safety and quality by better understanding the relationship between temperature, time, and electrical variables. This study seeks to deepen the understanding of the interaction mechanisms between food, packaging, and processing associated with this innovative technology. To accomplish this, the packaging was thoroughly characterized both before and after undergoing different OH treatments, ensuring a comprehensive evaluation of the structural and performance changes.

Materials and methods

Materials

In this study, we focused on evaluating a metallized multilayer film, specifically PET_{met}/PE (11/44 µm) (Finepack, São Paulo, Brazil). This film is widely utilized in the packaging of thermo-processed products, including sauces, pulps, and purées of fruits and vegetables. Additionally, sodium chloride from Sigma-Aldrich (USA), with a purity greater than 99%, and distilled water were utilized to prepare the food simulant.

Packaging sample preparation, model foods and ohmic heating processing

Flexible packaging samples measuring 80 mm × 220 mm were filled with 120 mL of a 0.1% (w/v) sodium chloride solution, which displayed an electrical conductivity of 1613 ± 45 µs cm^{-1} at 23 ºC. The rectangular shape of the packaging was specifically selected to enhance the distribution of electrical potential and promote uniform heating [19].

Ohmic heating processing was performed based on previous research [21], using two stainless steel electrodes placed at the interior side ends of the package. A function generator (1 Hz–25 MHz and 1–10 V; Agilent 33220 A, Penang, Malaysia) connected to a power amplifier system (4505 Precision Power Amplifier; Miko-Kings Instruments Ltd, Hong Kong, China) was employed to control the supplied voltage and, consequently, the temperature. Two distinct electrical frequencies—20 kHz and 50 Hz—were applied, creating an electric field intensity of approximately 3.7 V cm^{-1}, until the target treatment temperature of 80 °C was attained. A type K thermocouple, positioned at the geometric center of the sample volume, was utilized to monitor the temperature. Once the target temperature was reached, the samples were held at 80 °C for 5, 10, and 15 min, after which the sodium chloride solution was removed. It is noteworthy that the OH processing conditions used in this study different from those previously applied in [21], where, in this study, we explored different frequencies and longer exposure times to the treatment.

For each OH condition, ten packaging samples were processed. The treatments were categorized as follows: control (unprocessed samples), 20 kHz/5 min, 20 kHz/10 min, 20 kHz/15 min, 50 Hz/5 min, 50 Hz/10 min, and 50 Hz/15 min. The various samples were characterized both before and after OH processing regarding their morphology and structure (using SEM, FT-IR, and XRD), thermal properties (DSC), mechanical properties (tensile strength and seal strength), and barrier properties (to oxygen and water vapor), according to the methods outlined below.

Characterization of metallized packaging

Fourier-transform infrared (FT-IR) spectroscopy

FT-IR analysis was performed using a Fourier transform infrared spectrometer (Bruker, Alpha II, Billerica, USA) fitted with an attenuated total reflectance (ATR) attachment. The spectra of the outer and inner layers of the samples were recorded in the range of 4000 to 600 cm^{-1}, with a spectral resolution of 4 cm^{-1}, averaging 24 scans per measurement. The spectra were corrected and normalized relative to the baseline. To account for potential sample inhomogeneity and measurement variability, three spectra were recorded at different locations on each sample/layer [25, 26].

Differential scanning calorimetry (DSC)

The thermal characteristics of the packaging samples were evaluated before and after OH processing using a differential scanning calorimeter (DSC 6000, Perkin Elmer, Waltham, USA). About 5 mg of each sample was measured and placed in aluminum pans. The temperature was increased from 40 °C to 300 °C at a steady rate of 10 °C/min, while maintaining a nitrogen gas flow rate of 20 mL/min. DSC measurements were performed to determine the melting temperature (T_m) and melting enthalpy (ΔH) of the films. The results presented were the average of three repetitions [27].

X-ray diffraction (XRD)

X-ray diffraction patterns for all films were collected using an XRD system (Bruker D8, Odelzhausen, Germany). The

diffractometer utilized Cu-Kα radiation (λ = 1.54056 Å, 40 kV, 40 mA) and operated at a scan rate of 0.0333°/s. Diffraction intensity was measured as a function of the scattering angle, ranging from 10º to 30° with a step size of 0.04° and a scan duration of 1.2 s per step. The XRD patterns were analyzed to determine the overall crystallinity percentage using the free software Fityk, which calculates the ratio of the area under the peaks (indicating crystalline regions) to the total area (including both crystalline and amorphous regions) through peak deconvolution. The areas under the curves were determined via numerical integration. This method enhances the understanding of structural changes related to crystallinity, allowing for correlations with mechanical and barrier properties changes in the films before and after OH processing.

Scanning electron microscopy (SEM)

To investigate the morphology of the films' inner surface, samples were analyzed using scanning electron microscopy with an ultra-high-resolution field emission gun (FEG-SEM) (NOVA 200 Nano SEM, FEI Company). Topographic images were obtained with a secondary electron detector at an acceleration voltage of 10 kV, and SEM images were examined at a magnification of 5000×. Prior to the analysis, the samples were coated with a thin film (5 nm) of Au-Pd (80 − 20% by weight) using a high-resolution sputter coater (208 h Cressington Company), coupled with a MTM-20 Cressington (Cressington Company) high-resolution thickness controller.

Mechanical properties

Mechanical tests were conducted after conditioning the samples at 23 ± 2 °C and 50 ± 5% relative humidity (RH) for a minimum of 48 h. Samples measuring 25.4 mm in width were evaluated in both the machine direction (MD) and the transverse direction (TD). The tensile strength and seal strength properties were measured using a universal testing machine (Instron, 5966-E2, Norwood, USA). Tensile strength was assessed with a 100 N load cell at a testing speed of 50 mm/min, using an initial gauge length of 40 mm for the MD and 100 mm for the TD [28]. Seal strength was tested until failure with a 1 kN load cell at a speed of 300 mm/min, starting with a 10 mm gap for both directions [29]. All tests were performed in five replicates.

Water vapor and oxygen barrier properties

Water vapor transmission rates (WVTR) and oxygen transmission rates (OTR) were determined using PERMATRAN equipment (3/34 G, MOCON, Minneapolis, USA) with an infrared sensing device for WVTR, and OXTRAN equipment (2/22 H, MOCON, Minneapolis, USA) for OTR. The permeation area for both measurements was 5 cm^2. The WVTR was evaluated at 38 °C and 90% RH, while the OTR was determined at 23 °C in a dry environment, with the outer surface of the sample exposed to the permeant gas (100% O_2). Readings were adjusted for a partial pressure gradient of the 1 atm permeant gas [30, 31].

Statistical analysis

The results are displayed as mean ± standard deviation and were statistically analyzed using analysis of variance (ANOVA), followed by Tukey's test to compare the average values of packaging properties before and after OH treatment, with a significance level established at 0.05.

Results and discussion

Fourier-transform infrared spectroscopy (FT-IR)

Figure 1 displays the FT-IR spectra of the outer PET layer and the inner PE layer before and after OH treatment. The primary FT-IR peaks for PET molecules are illustrated in Fig. 1(a). The peak at 1714 cm^{-1} corresponds to the C = O stretching vibrations, indicative of the carbonyl groups present in the polymer. The peaks at 1578 cm^{-1} and 1505 cm^{-1} correspond to the aromatic vibrations associated with C = C stretching. Peaks between 1470 cm^{-1} and 1330 cm^{-1} correspond to the deformation stretching of the CO group and the bending and rocking vibrational modes related to the ethylene glycol segment of the PET structure. The peak at 1244 cm^{-1} is indicative of the terephthalate group, while the peaks at 1097 cm^{-1} and 1045 cm^{-1} correspond to the methylene group and vibrations of the CO ester bond. Additionally, the range of 1017 to 720 cm^{-1} represents the vibrations of the aromatic rings [32, 33].

Figure 1(b) shows the FT-IR peaks for PE molecules, with the peaks at 2915 cm^{-1} and 2849 cm^{-1} corresponding to the asymmetric and symmetric stretching vibrations of CH_2, respectively. The FT-IR peak at 1471 cm^{-1} is associated with CH deformation vibrations in CH_2 and the peak at 717 cm^{-1} corresponds to the C-C equilibrium vibrations in CH_2 [34–37].

The FT-IR results indicated a small, and not relevant, difference in the FT-IR spectra of PET and PE after applying different OH processing conditions, regardless of the electrical frequency and exposure time used. This indicates that the OH conditions do not change the surface chemistry of the polymers (PET and PE) used in the packaging.

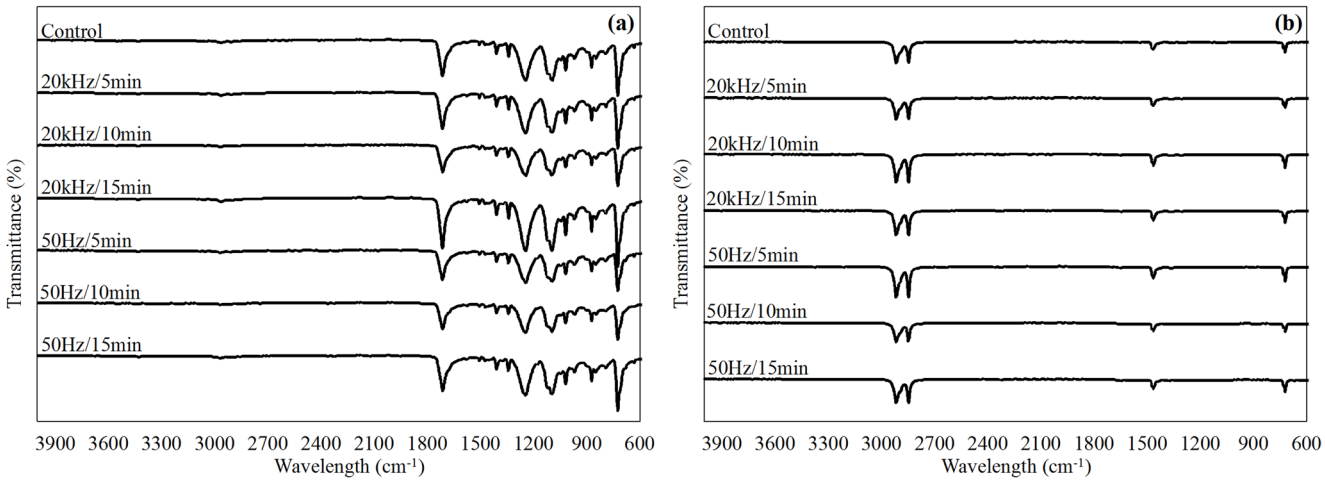


Fig. 1 FT-IR spectra for the outer layer of PET (**a**) and the inner layer of PE (**b**) from the packaging processed under various OH conditions.

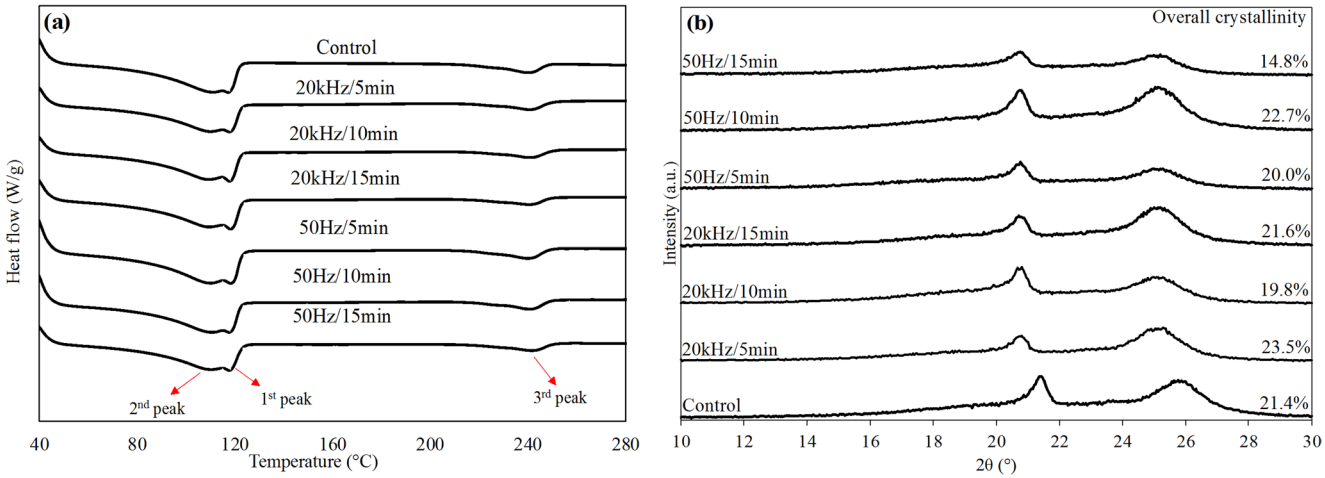


Fig. 2 Differential Scanning Calorimetry (DSC) results (**a**) and X-ray diffraction patterns (**b**) for the packaging subjected to various OH processing conditions.

Table 1 DSC analysis of the packaging subjected to various OH processing conditions.

Sample	Thermal property			
	T_m (°C) 1st peak	T_m (°C) 2nd peak	T_m (°C) 3rd peak	ΔH* (J/g)
Control	110.2±2.5[a]	117.8±0.5[a]	240.0±0.6[a]	83.9±12.7[a]
20 kHz/5 min	110.1±0.8[a]	117.8±0.6[a]	241.7±1.4[a]	75.3±18.3[a]
20 kHz/10 min	109.6±0.8[a]	118.0±0.3[a]	241.2±0.4[a]	71.6±15.6[a]
20 kHz/15 min	109.7±1.7[a]	118.6±0.1[a]	240.1±2.1[a]	74.0±15.1[a]
50 Hz/5 min	109.5±1.2[a]	118.6±0.3[a]	240.4±1.4[a]	81.4±2.5[a]
50 Hz/10 min	110.6±1.2[a]	117.8±0.4[a]	241.2±0.4[a]	79.3±2.1[a]
50 Hz/15 min	111.0±2.6[a]	118.5±1.2[a]	242.3±1.5[a]	70.2±12.8[a]

T_m: melting temperature and ΔH*: total enthalpy of melting Values referring to the mean of three replicates±standard deviation. [a, b,c] means followed by the same letter in the column do not differ at the 95% confidence level ($p<0.05$)

Differential scanning calorimetry (DSC)

The differential scanning calorimetry (DSC) curves for the multilayer films before and after OH processing are presented in Fig. 2(a). The main parameters obtained from the DSC analysis for the films are summarized in Table 1. The DSC curve for the PET_{met}/PE film showed three melting peaks (T_m). The first peak was associated with LDPE, the second with LLDPE, and the third with PET. The T_m values were between 109.5 ºC and 111.0 ºC for LDPE, 117.8 ºC and 118.6 ºC for LLDPE, and 240.0 ºC to 242.3 ºC for PET. These values are consistent with those found in the literature for these polymers [22, 35, 38, 39]. The total enthalpies of melting (ΔH) values ranged from 70.2 J/g to 83.9 J/g.

The T_m and ΔH results were not significantly affected by the OH processing, indicating that the electrical frequency and processing time conditions do not alter the thermal characteristics of the polymers the comprise the packaging.

These results align with the FT-IR findings, indicating that the OH conditions used do not significantly change the chemical structure or thermal properties of the tested polymers.

X-ray diffraction (XRD)

Figure 2(b) shows the X-ray diffraction patterns and overall crystallinity percentages of PET_{met}/PE films before and after OH processing under different conditions. The crystallinity was measured using peak separation, and background noise from the instrument was carefully removed prior to calculations to ensure accuracy. The films exhibited two crystalline peaks at the angular positions of 2θ = ~26° and ~21°, which are associated with the semi-crystalline structures of PET and PE [40].

The control PET_{met}/PE film displayed an overall crystallinity value of 21.4%. After being processing by OH at 50 Hz for 15 min, the overall crystallinity decreased to 14.8%. It is possible that this decrease may be related to the breakdown of polymer chains due to the low-frequency OH treatment, which could affect the structural organization. These results indicated that processing with low frequency, high temperature, and extended exposure time negatively affected the crystallinity of the films. The use of low frequency may lead to the formation of radical species due to electrochemical reactions, potentially altering the material´s properties. However, the results were similar to those found in multilayer flexible packaging exposed to longer durations (≥15 min) using conventional heating and microwave-assisted thermal sterilization [41].

For the other OH processing conditions, the overall crystallinity values ranged from 19.8 to 23.5%. These variations, roughly 2% in comparison to the control sample, indicate that the other processing conditions had a relatively negligible effect on the overall crystallinity of the films when contrasted with the OH condition of 50 Hz for 15 min.

Film surface morphology

Figure 3 presents scanning electron microscopy (SEM) images showcasing the surface morphologies of the inner layers of both control and OH-processed PET_{met}/PE films. The inner layer was chosen for analysis because it is in direct contact with the food simulant and is relevant to the configuration of the OH processing, which positioned the electrodes within the packaging. The surfaces of the samples exhibited a characteristic roughness typical of PE films [42]. Following the application of different OH conditions, the samples showed an increased surface roughness along with presence of small inclusions. These alterations may be attributed to the high-temperature conditions, extended processing time, and the interaction between the material and the food simulant [21, 39]. Additionally, these minor changes to the internal surfaces of the films correlate with the variations observed in the overall crystallinity, as demonstrated in Fig. 2(b). It is important to note that both the changes in overall crystallinity and the surface morphology of the films can significantly impact the mechanical and barrier performance of the packaging, and these aspects will be further discussed in the subsequent sections.

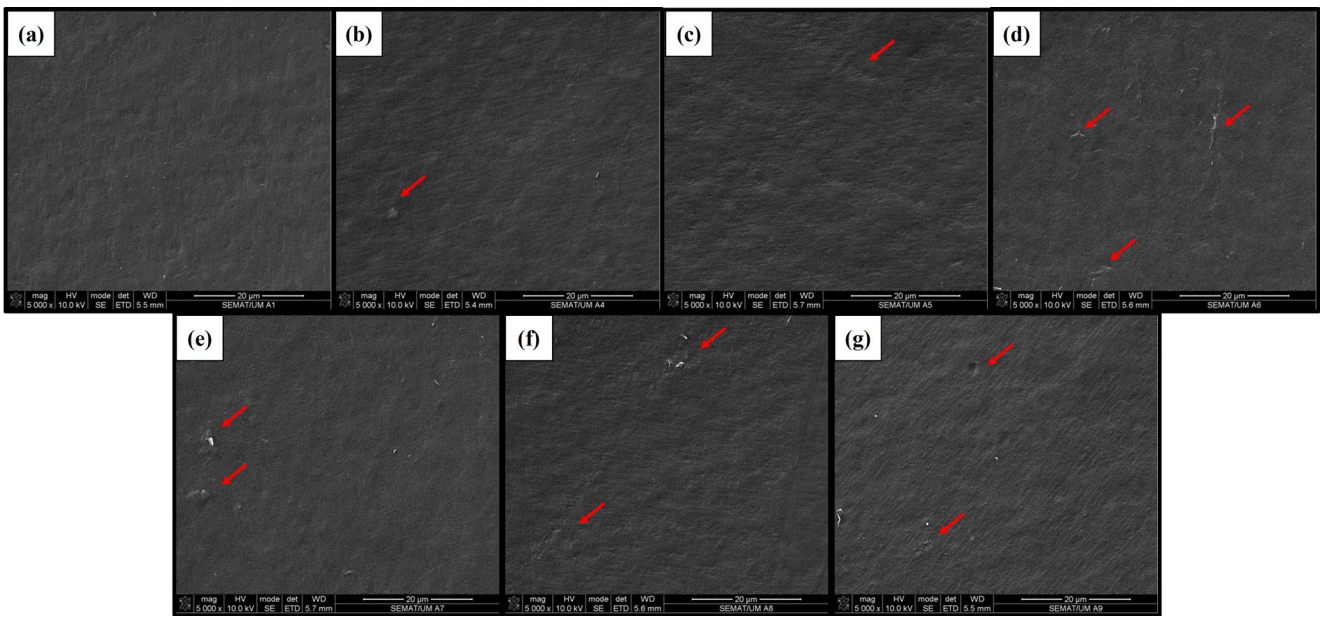


Fig. 3 Scanning electron microscopy images of the inner surface of packaging subjected to various OH processing conditions. (**a**) control, (**b**) 20 kHz/5 min, (**c**) 20 kHz/10 min, (**d**) 20 kHz/15 min, (**e**) 50 Hz/5 min, (**f**) 50 Hz/10 min and (**g**) 20 Hz/15 min.

Mechanical properties

Figure 4 displays the results of tensile strength (TS), elongation at break (EB), and maximum seal strength for PET_{met}/PE films, illustrating changes in both the machine direction (MD) and transverse direction (TD) before and after the application of various OH processing conditions.

The TS values ranged from 42.3 MPa to 51.3 MPa in the MD and from 49.1 MPa to 53.9 MPa in TD. The samples treated at 50 Hz for 5 min exhibited significantly higher TS values in MD compared to the other samples (Fig. 4(a)). In the TD, the sample processed at 20 kHz for 15 min demonstrated a significantly higher TS value than the control sample (Fig. 4(b)). Regarding EB, OH processing did not lead to significant changes in the MD when compared to the control (Fig. 4(c)). However, there was a notable reduction in the EB of the samples treated at 20 kHz for 5 min when compared to the control sample, although this sample did not differ significantly from the other OH-processed samples (Fig. 4(d)). No discernible trends in these properties (TS and EB) were observed based on frequency or processing time, complicating the interpretation of the minor increases seen in specific samples. Moreover, the TS values obtained for all films fall within the ranges commonly reported in the literature for metallized films [22, 43]. In conclusion, the applied OH conditions do not negatively impact the TS and EB of the packaging, indicating a positive result for the use of this material in OH technology.

The PET_{met}/PE multilayer materials exhibited maximum seal strength values ranging from 4.3 kgf 25.4 mm^{-1} to 7.6 kgf 25.4 mm^{-1} in MD and from 4.2 kgf 25.4 mm^{-1} to 5.3 kgf 25.4 mm^{-1} in TD. These results fall within the values reported in the literature for sealing layer composed of PE films or coatings [22, 44]. After OH processing, the samples treated at 20 kHz for 10 min and 50 Hz for 15 min showed a significant reduction in maximum seal strength in the MD compared to the control sample. These findings correlate with the overall crystallinity results presented in Fig. 2(b), which indicated that these samples had the lowest crystallinity values. Thus, the reduction in crystallinity caused by OH processing negatively impacted the maximum seal strength of the films. However, no consistent trends in reduction were observed based on frequency or processing time. Additionally, these reductions were not observed in the TD, likely because this direction undergoes less stretching during film production, consequently resulting in a reduced negative impact. It is important to note that, despite some samples exhibiting a reduction in maximum sealing strength, no leaks were detected, indicating that the integrity of the packaging was maintained. This outcome is therefore viewed as a positive result.

Barrier properties

The water vapor transmission rate (WVTR) and oxygen transmission rate (OTR) results of the PET_{met}/PE films before and after the applying various OH conditions are presented in Fig. 5. The WVTR values ranged from 2.00 ± 0.19 $g.m^{-2}.day^{-1}$ to 3.21 ± 0.53 $g.m^{-2}.day^{-1}$, while the OTR values ranged from 4.08 ± 0.16 $mL_{(STP)}.m^{-2}.day^{-1}$ to 5.14 ± 1.27 $mL_{(STP)}.m^{-2}.day^{-1}$. These results fall within the ranges reported in the literature for PET_{met}/PE films [21, 45].

The different OH processing conditions applied did not significantly affect the barrier properties of the materials, which is a positive outcome for the application of this material in this technology. Despite some surface irregularities and changes in crystallinity, no alterations in the metallization of the film were observed, as seen in Fig. 3, which likely contributed to the maintenance of the barrier properties of this packaging material. Additionally, due to the hydrophobic nature of polyethylene, the processing had no discernible impact on the interaction of the material with the aqueous food simulant used [40, 46]. Therefore, this material is an excellent candidate for processing food within the packaging using OH technology, as the preservation of barrier properties during processing would certainly help maintain food quality during storage.

Conclusions

The metallized multilayer flexible packaging was processed under OH pasteurization conditions utilizing different electrical frequencies and processing times. The evaluations of chemical structure via FT-IR, thermal behavior through DSC, and barrier properties for water vapor and oxygen demonstrated that the film remained stable irrespective of the applied OH conditions. This is a positive outcome for the potential application of this material in such technology. Notably, the tested conditions align with those frequently reported in the scientific literature and used in industrial practices, supporting their relevance as realistic processing scenarios. However, OH processing did lead to some changes in crystallinity, the surface of the inner layer, and mechanical properties, including tensile and seal strength. Although the applied OH conditions resulted in some modifications to the materials, these changes were minimal and sporadic, without displaying a distinct trend. Therefore, the food-packaging-process interactions identified in this research do not negatively affect the use of this material. Ultimately, PET_{met}/PE films can be effectively used to package foods that will undergo the OH processing conditions investigated in this study. This could help reduce costs

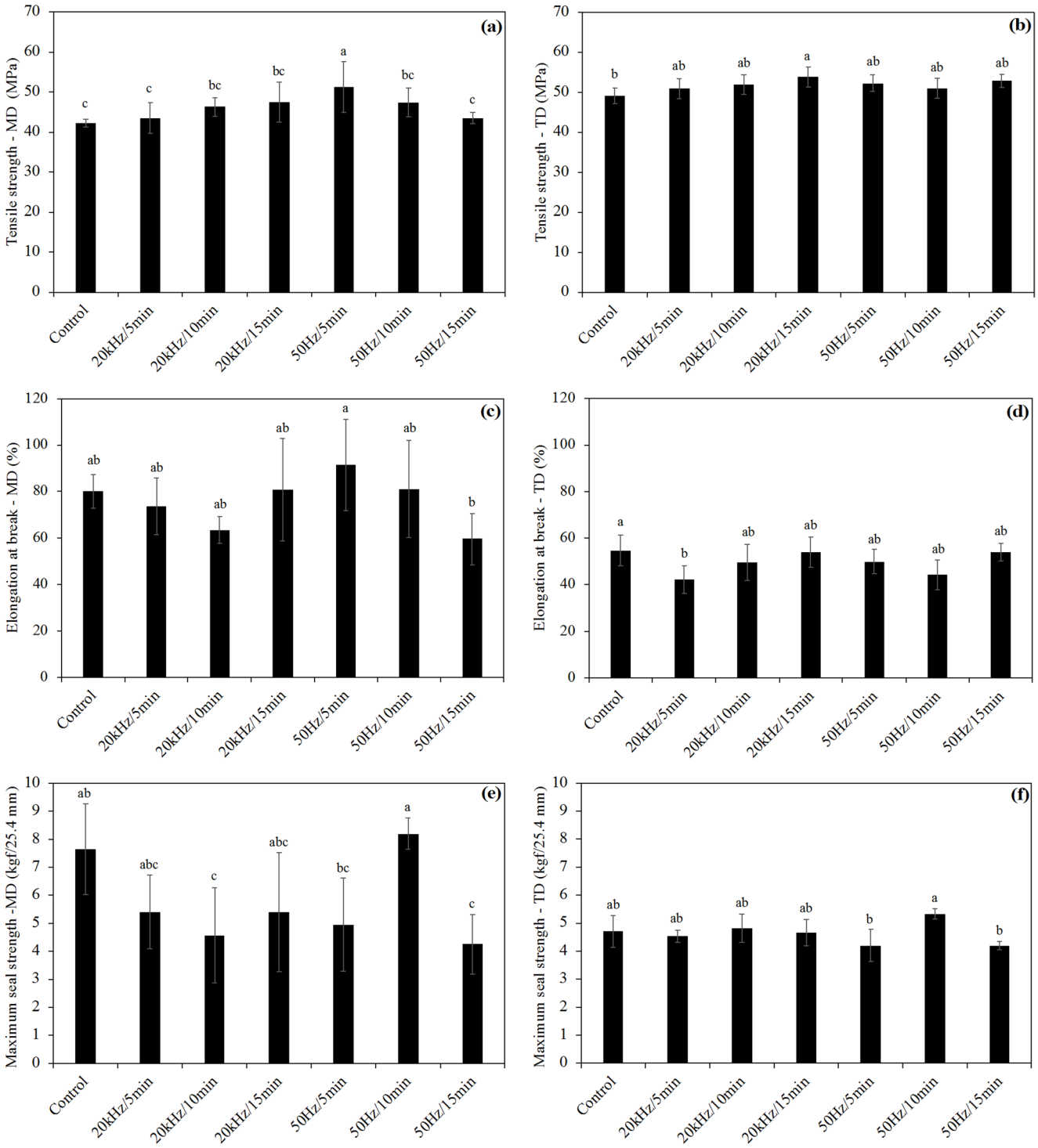


Fig. 4 Tensile strength (**a**, **b**), elongation at break (**c**, **d**), and maximum seal strength (**e**, **f**) of the packaging treated under various OH conditions. MD: machine direction; TD: transverse direction. Values marked with the same lowercase letters (MD) or uppercase letters (TD) are not significantly different at the 95% confidence level ($p < 0.05$).

associated with aseptic systems and potentially extend product shelf life, providing a viable alternative for processing and packaging products directly within the package.

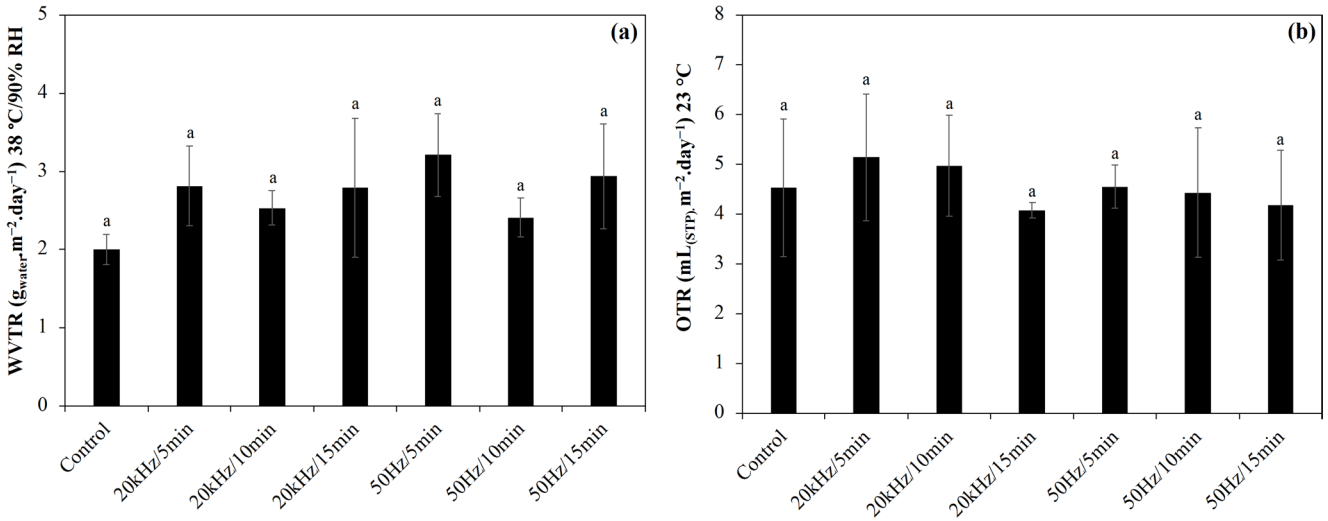


Fig. 5 WVTR (**a**) and OTR (**b**) of the packaging processed by different OH conditions. The same lowercase letters do not differ at the 95% confidence level ($p < 0.05$).

Acknowledgements This study was partly funded by the Coordination for the Improvement of Higher Education Personnel– Brazil (CAPES)– Financial Code 001. The authors would like to thank the *Fundo de Apoio ao Ensino*, *Pesquisa e Extensão*– FAEPEX of UNICAMP for the Early Career Grant No. 2978/24. The authors wish to express their acknowledgment to the São Paulo Research Foundation (FAPESP) for supporting post-doctoral fellowship (grant #2022/09587-3). They also acknowledge the funding received for the Multi-user Equipment Program (grant #2021/04043-2), as well as grants #2018/15758-0 and #2018/15759-6, and the State Research Institutes Modernization Program (grant #2017/50349-0). Additionally, Ricardo N. Pereira thanks the FCT for the Assistant Research Program, specifically regarding the Scientific Stimulus Employment reference CEECIND/02903/2017 (doi:https://doi.org/10.54499/CEECIND/02903/2017/CP1458/CT0006).

Author contributions Conceptualization, Validation, Formal analysis, Methodology, Investigation, Data curation, Formal analysis, Resources, Funding acquisition, Writing– original draft. ***R. M. Rodrigues***: Conceptualization, Validation, Methodology, Formal analysis, Writing - Review & Editing. ***R. N. Pereira***: Conceptualization, Validation, Methodology, Formal analysis, Writing - Review & Editing. ***D. Ito***: Investigation, Methodology, Writing - Review & Editing. ***F. T. Gomes***: Investigation, Methodology, Writing - Review & Editing. ***M. Padula***: Conceptualization, Validation, Supervision, Resources, Funding acquisition, Writing– review & editing. ***A. A. Vicente***: Conceptualization, Validation, Supervision, Resources, Funding acquisition, Writing– review & editing.

Declaration

Conflict of interest The authors affirm that they have no known competing financial interests or personal relationships that may have influenced the outcomes reported in this paper.

References

1. L. Marangoni Júnior, C.A.R. Anjos, M. Cristianini, *High Pressure Thermal Processing* (Elsevier, 2023), pp. 269–289
2. D. Hygreeva, M.C. Pandey, Trends Food Sci. Technol. **54**, 175 (2016)
3. R.S. Rocha, R. Silva, J.T. Guimarães, C.F. Balthazar, T.C. Pimentel, R.P.C. Neto, M.I.B. Tavares, E.A. Esmerino, M.Q. Freitas, L.P. Cappato, R.N. Calvacanti, F.N. Rodrigues, R.S.L. Raices, M.C. Silva, A.G. Cruz, Food Res. Int. **131**, 109027 (2020)
4. R.S. Rocha, R. Silva, G.L.P. Ramos, L.A. Cabral, T.C. Pimentel, P.H. Campelo, P. Blumer Zacarchenco, M.Q. Freitas, E.A. Esmerino, M.C. Silva, A.G. Cruz, Food Res. Int. **161**, 111827 (2022)
5. R. Silva, R.S. Rocha, J.T. Guimarães, C.F. Balthazar, T.C. Pimentel, R.P.C. Neto, M.I.B. Tavares, E.A. Esmerino, M.C.K.H. Duarte, M.Q. Freitas, P.H.F. Silva, L.P. Cappato, R.S.L. Raices, M.C. Silva, A.G. Cruz, Innovative Food Sci. Emerg. Technol. **65**, 102475 (2020)
6. A. Iqbal, A. Murtaza, W. Hu, I. Ahmad, A. Ahmed, X. Xu, Food Bioprod. Process. **117**, 170 (2019)
7. R.P.S. Pires, L.P. Cappato, J.T. Guimarães, R.S. Rocha, R. Silva, C.F. Balthazar, M.Q. Freitas, P.H.F. Silva, R.P.C. Neto, M.I.B. Tavares, D. Granato, R.S.L. Raices, M.C. Silva, A.G. Cruz, J. Food Eng. **280**, 109989 (2020)
8. H.A. Makroo, N.K. Rastogi, B. Srivastava, Trends Food Sci. Technol. **97**, 451 (2020)
9. E.-R. Cho, D.-H. Kang, Food Res. Int. **179**, 113978 (2024)
10. O.Y. Barrón-García, E. Morales-Sánchez, A.K. Ramírez Jiménez, M. Antunes-Ricardo, I. Luzardo-Ocampo, E. González-Jasso, and M. Gaytán-Martínez, Food Research International 154, 111032 (2022)
11. L.P. Cappato, M.V.S. Ferreira, J.T. Guimaraes, J.B. Portela, A.L.R. Costa, M.Q. Freitas, R.L. Cunha, C.A.F. Oliveira, G.D. Mercali, L.D.F. Marzack, A.G. Cruz, Trends Food Sci. Technol. **62**, 104 (2017)
12. M. Gavahian, Y. Chu, S. Sastry, Compr. Rev. Food Sci. Food Saf. **17**, 1040 (2018)
13. C.M. Knirsch, C.A. Santos, A.A.M. de Vicente, T.C.V. Pena, Trends Food Sci. Technol. **21**, 436 (2010)
14. T.C.P. Moreira, R.N. Pereira, A.A. Vicente, R.L. Cunha, Food Research International 116, 628 (2019)
15. P. Inmanee, P. Kamonpatana, T. Pirak, LWT. **108**, 183 (2019)
16. C. Tiravibulsin, Y. Lorjaroenphon, P. Udompijitkul, P. Kamonpatana, LWT. **147**, 111552 (2021)
17. K. Kanogchaipramot, K. Tongkhao, T. Sajjaanantakul, P. Kamonpatana, J. Food Sci. **81**, (2016)

18. P. Kamonpatana, *Packaging for Foods Processed by Ohmic Heating* (Elsevier, 2018)
19. R. Somavat, P. Kamonpatana, H.M.H. Mohamed, S.K. Sastry, J. Food Eng. **112**, 134 (2012)
20. S. Jun, S. Sastry, J. Food Eng. **80**, 1199 (2007)
21. L. Marangoni Júnior, R.M. Rodrigues, R.N. Pereira, P.E.D. Augusto, D. Ito, F.G. Teixeira, M. Padula, A.A. Vicente, Food Chem. **456**, 140038 (2024)
22. L. Marangoni Júnior, L.M. de Oliveira, F.B.H. Dantas, M. Cristianini, M. Padula, C.A.R. Anjos, J. Food Eng. **273**, 109812 (2020)
23. L. Delva, C. Deceur, N. Van Damme, K. Ragaert, in (2019), p. 030005
24. I. Berkane, A. Cabanes, O. Horodytska, I. Aracil, A. Fullana, Resour. Conserv. Recycl. **189**, 106744 (2023)
25. ASTM-E1252-98, 13 (2021)
26. ASTM-E573-01, 17 (2021)
27. ASTM-D3418-21, 8 (2021)
28. ASTM-D882, 12p, (2018)
29. ASTM-F88/F88M, West, Conshohocken, ASTM. 1 (2023)
30. ASTM-F1249, 7 (2020)
31. ASTM-D3985, 7 (2017)
32. A.P. dos, S. Pereira, M.H.P. da Silva, É., P. Lima, A. Paula, F.J. Tommasini, Materials Research 20, (2017)
33. Z. Chen, J.N. Hay, M.J. Jenkins, Thermochim Acta. **552**, 123 (2013)
34. R. Kochetov, T. Christen, F. Gullo, in 2017 *1st International Conference on Electrical Materials and Power Equipment (ICEMPE)* (2017), pp. 49–52
35. L. Marangoni Júnior, P.E.D. Augusto, R.P. Vieira, D.F. Borges, D. Ito, F.G. Teixeira, F.B.H. Dantas, M. Padula, Food Res. Int. **163**, 112217 (2023)
36. B.B. Turriziani, R.P. Vieira, L. Marangoni, Júnior, R.M.V. Alves, J. Polym. Environ. (2023)
37. A.M. Elbasiony, A.I. Sharshir, M.M. Ghobashy, D.M. Alshangiti, M. Madani, S.A. Al-Gahtan, A.M.A. Henaish, M.M. Abdelhamied, Opt. Mater. (Amst). **148**, 114811 (2024)
38. A. Benítez, J.J. Sánchez, M.L. Arnal, A.J. Müller, O. Rodríguez, G. Morales, Polym. Degrad. Stab. **98**, 490 (2013)
39. L. Marangoni Júnior, L.M.D. Oliveira, P.F.J. Bócoli, M. Cristianini, M. Padula, C.A.R. Anjos, J. Food Eng. **276**, (2020)
40. B.B. Turriziani, M.Â.F. Perez, P.H.M. Kiyataka, R.P. Vieira, L. Marangoni, Júnior, R.M.V. Alves, J. Polym. Res. **30**, 194 (2023)
41. S. Dhawan, C. Varney, G.V. Barbosa-Cánovas, J. Tang, F. Selim, S.S. Sablani, J. Appl. Polym. Sci. **131**, (2014)
42. P.B. Jaiswal, B.K. Pushkar, K. Maikap, P.A. Mahanwar, Polym. Degrad. Stab. **206**, 110156 (2022)
43. M.J. Galotto, P.A. Ulloa, D. Hernández, F. Fernández-Martín, R. Gavara, A. Guarda, Packaging Technol. Sci. **21**, 297 (2008)
44. C. Ge, H.N. Cheng, N. Ribalko, C.A. Joshi, N. Strong, Food Packag Shelf Life. **40**, 101222 (2023)
45. F.B.H. Dantas, I.D. Alvim, A.M.R. de Miguel, R.M.V. Alves, L. Marangoni, Júnior, J. Packag Technol. Res. **6**, 225 (2022)
46. L. Marangoni, M.Â. Fávaro Perez, C.D. Torres, M. Cristianini, P.H. Massaharu Kiyataka, A.C. Albino, M. Padula, and C. A. Rodrigues Anjos, Food Packag Shelf Life 26, (2020)

Publisher's note Springer Nature remains neutral with regard to jurisdictional claims in published maps and institutional affiliations.

Springer Nature or its licensor (e.g. a society or other partner) holds exclusive rights to this article under a publishing agreement with the author(s) or other rightsholder(s); author self-archiving of the accepted manuscript version of this article is solely governed by the terms of such publishing agreement and applicable law.